AMSR-2 Air-Sea Essential Climate Variables
RSS Version 8.2

Frank J. Wentz

Remote Sensing Systems (RSS) has updated its AMSR-2 data processing from Version 8.0 to Version 8.2[note 1]. A mission-long (July 2012 to present) V8.2 dataset is now available. Version 8.2 is a major update, and we encourage all users, particularly those doing climate studies, to transition to the V8.2 dataset. Both V8.0 and V8.2 datasets will be available for a short overlap period TBD.

The two major changes for V8.2 are:
1. Spurious drifts in the AMSR-2 retrievals (SST, wind, vapor, cloud, and rain) have been removed.
2. The output data files are now in netCDF format.

This document discusses the spurious drift problem and subsequent correction.

Note 1: Version 8.1 was an in-house beta test not publicly released.

Remote Sensing Systems
www.remss.com

Drifts in the AMSR-2 Air-Sea Essential Climate Variables (AS-ECV)

The AMSR-2 Air-Sea Essential Climate Variable (AS-ECV) Climate Record begins with the launch of AMSR-2 in July 2012 and is currently about 9 years in length. The climate variables that make up this record are:

- ➤ Sea-Surface Temperature (SST, C)
- ➤ Near-Surface Wind Speed (m/s)
- ➤ Atmospheric Columnar Water Vapor (mm)
- ➤ Atmospheric Columnar Cloud Water (mm)
- ➤ Sea-Surface Rain Rate (mm/hr)

The RSS 2020 Assessment of operational satellite microwave radiometers (AMSR-2, WindSat, GMI, SSM/IS) revealed drifts in AMSR-2 AS-ECV timeseries.

This document describes the characterization and removal of the these drifts. A complete reprocessing of the AMSR-2 mission data has been performed and will be distributed as Version 8.2.

Remote Sensing Systems
www.remss.com

Characterization of Long-Term Drifts in V8.0 AMSR-2 AS-ECVs

The following slides show the drifts in the V8.0 AMSR-2 AS-ECVs.

Figure 1 compares the AMSR-2 AS-ECVs with those from two other satellite microwave radiometers: WindSat and GMI. The drift in SST and wind is obvious. The cloud water also exhibits a drift relative to WindSat and GMI. Results are shown for both V8.0 (before drift correction) and the newly released Version 8.2.

Figure 2 shows the timeseries of the difference of the AMSR-2 SST minus the Reynolds SST and the CMC SST. Results are shown for both V8.0 (before drift correction) and the newly released Version 8.2.

Figure 3 shows the timeseries of the V8.0 AMSR-2 SST minus buoy SST.

Figure 4 shows the V8.0 AMSR-2 wind speed compared to wind retrievals from the ASCAT-B satellite scatterometer.

Conclusion: There is no doubt that the V8.0 AMSR-2 AS-ECVs are drifting.

3

Remote Sensing Systems
www.remss.com
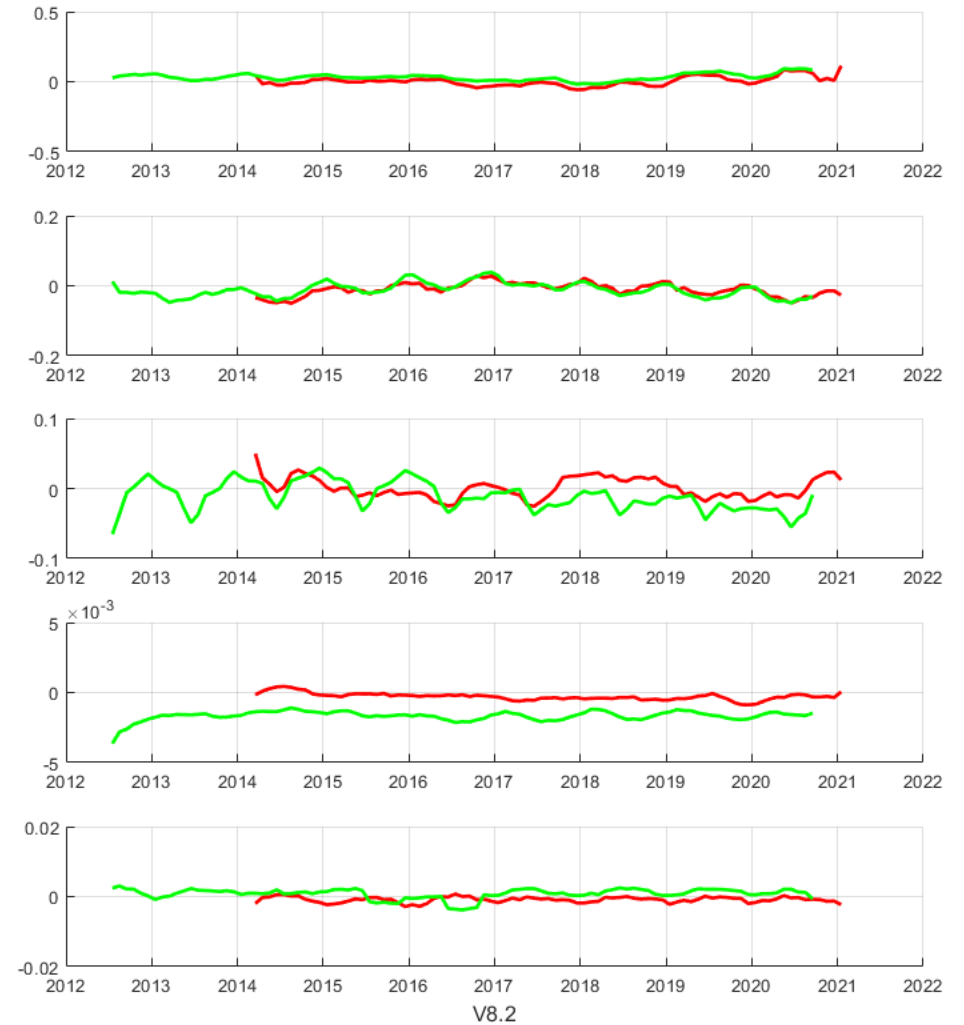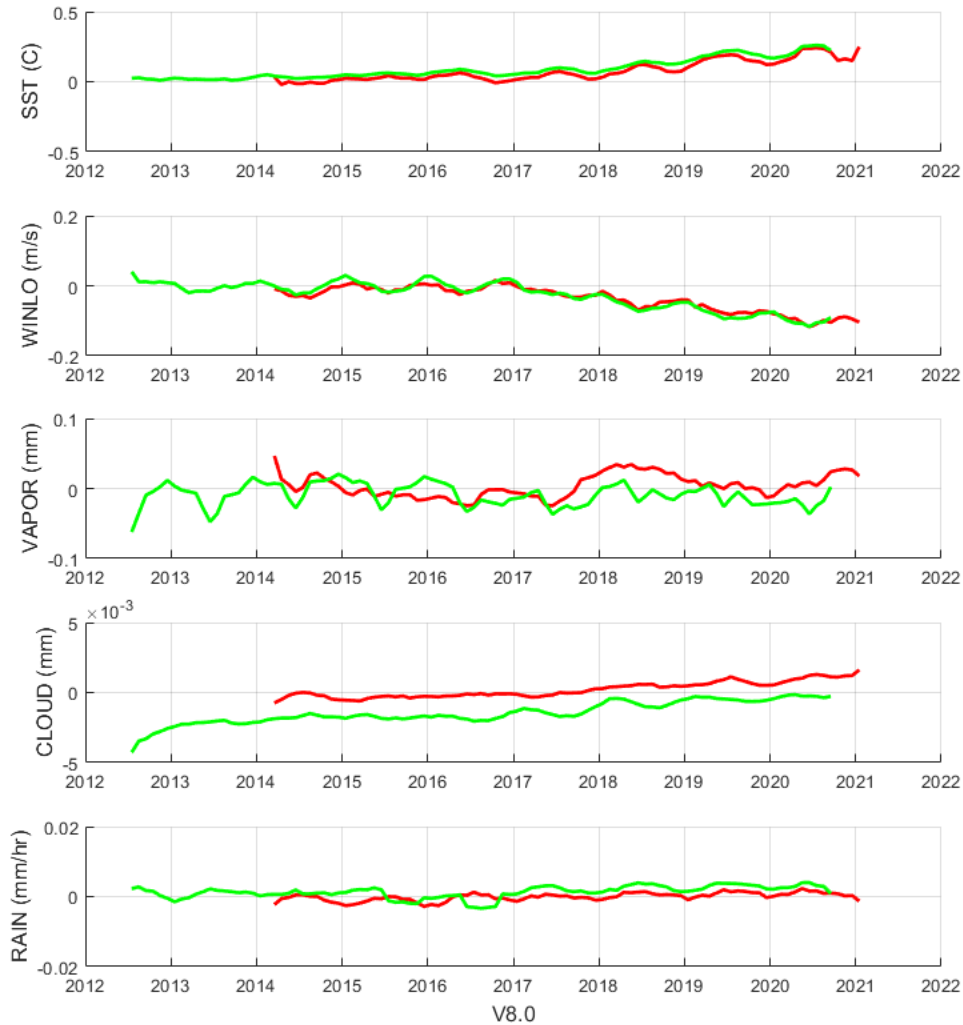
Fig. 1. Timeseries showing the difference of the AMSR-2 AS-ECVs minus similar retrievals from WindSat (green curve) and GMI (red curve). The left column shows the obvious drift in the V8.0 product and the right column shows the new V8.2 product with the drifts removed. Seasonal variations in AMSR2 − WindSat curves are probably due to the large difference in the local ascending node time between these two sensors.

Remote Sensing Systems
www.remss.com
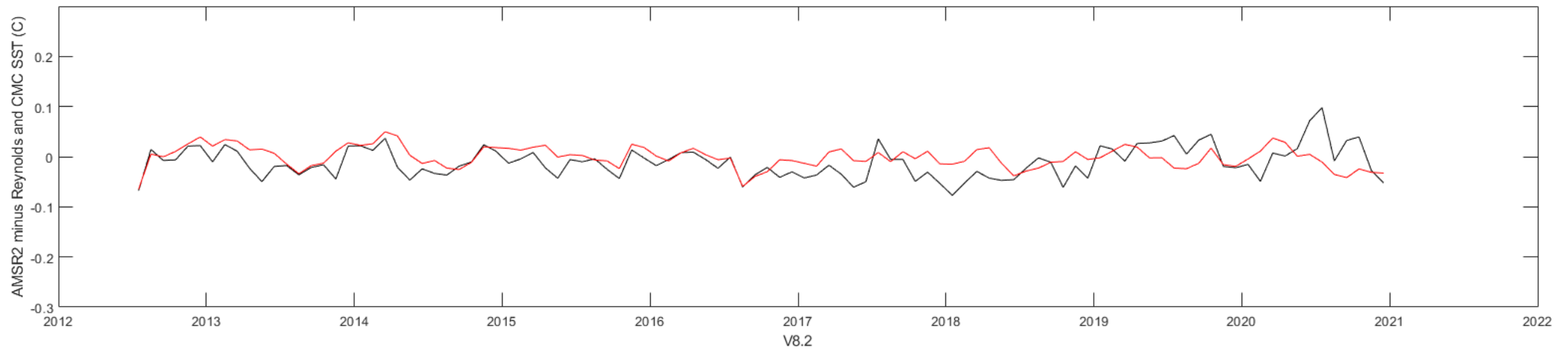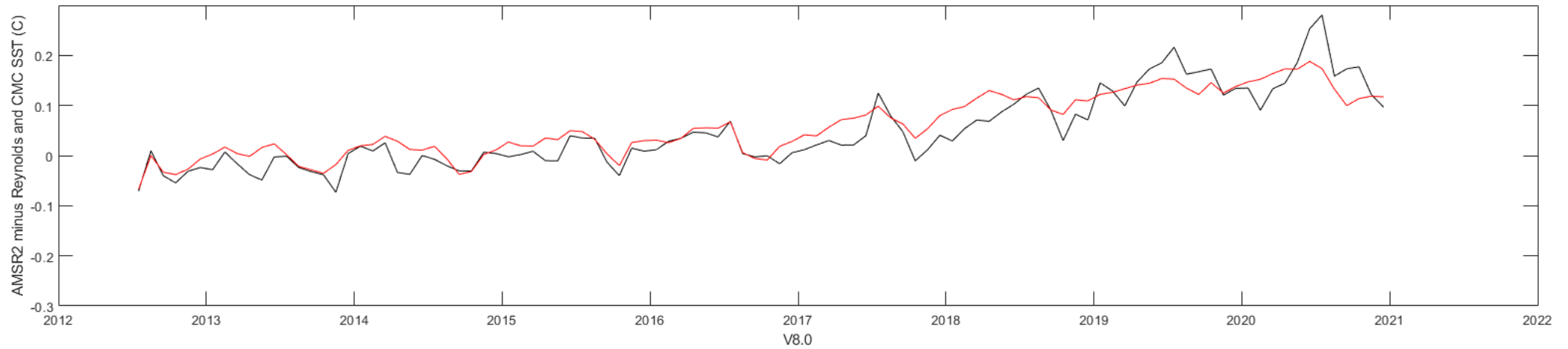
Fig. 2. Timeseries showing the difference of the AMSR-2 SST minus Reynolds SST (black curve) and CMC SST (red curve). The top frame shows the obvious drift in the V8.0 product, and the bottom frame shows the new V8.2 product with the drifts removed.

Remote Sensing Systems
www.remss.com
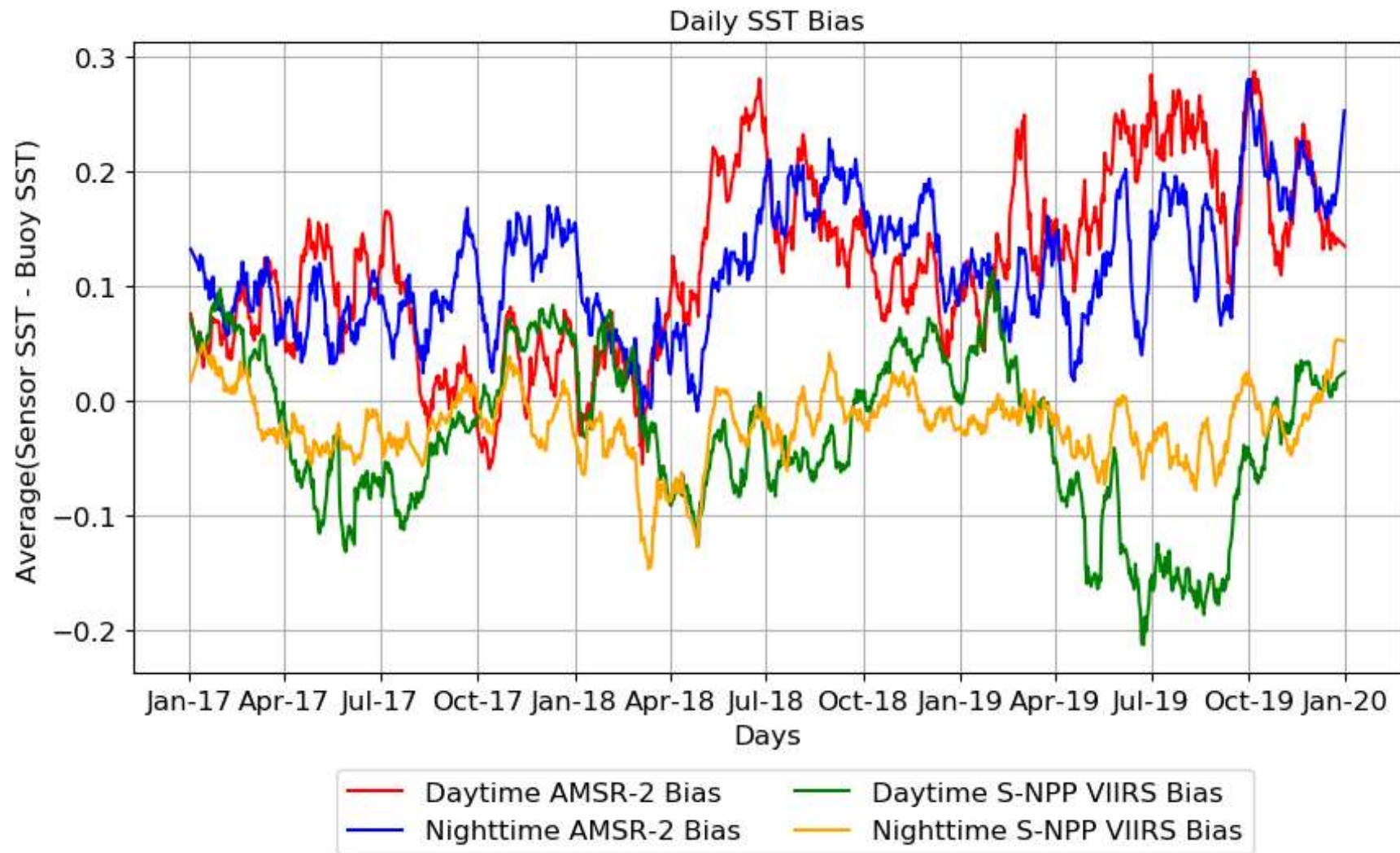
Fig. 3. These timeseries show the difference of the AMSR-2 SST minus buoy SST for both day and nighttime passes (red and blue curves, respectively). These results are for V8.0 before the drift correction.
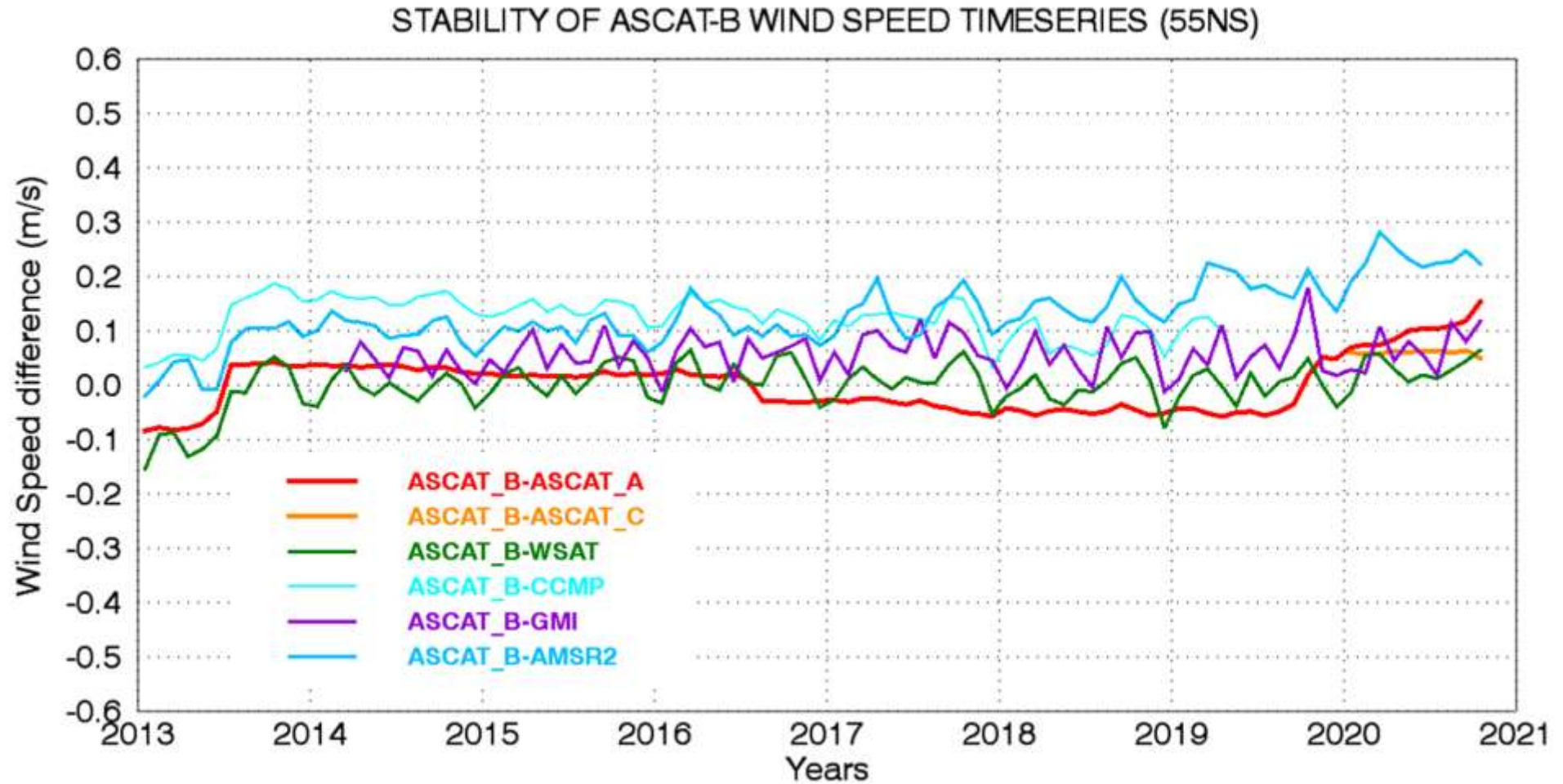
Remote Sensing Systems
www.remss.com

STABILITY OF ASCAT-B WIND SPEED TIMESERIES (55NS)

Legend:
- ASCAT_B-ASCAT_A (red)
- ASCAT_B-ASCAT_C (orange)
- ASCAT_B-WSAT (green)
- ASCAT_B-CCMP (cyan)
- ASCAT_B-GMI (purple)
- ASCAT_B-AMSR2 (blue)

Fig. 4. These timeseries show the difference between the ASCAT-B wind speed and various other satellites. The difference between ASCAT-B and AMSR-2 is shown by the cyan curve. These results are for V8.0 before the drift correction. This shows the AMSR-2 wind speed decreasing with time over the 8-year period.

Remote Sensing Systems
www.remss.com

Relating Drifts in AMSR-2 AS-ECVs to Drifts in Antenna Temperatures

We used our Ocean Radiative Transfer Model (ORTM) to convert the drifts in the AS-ECVs to drifts in the AMSR-2 Antenna Temperatures (TA). In doing this, we assume the AS-ECV drifts are a linear function of time. Based on the results shown in Figure 1, we model the AS-ECV drifts as linear functions of time with the following slopes:

SST:	0.28 C per decade
Wind:	0.14 m/s per decade
Vapor:	0.024 mm per decade
Cloud:	0.0029 mm per decade

Figures 5 and 6 show the timeseries of the difference of the AMSR-2 TA measurement minus the ORTM TA for V-pol and H-pol, respectively. In computing the ORTM TA we use the AMSR-2 wind, vapor, and cloud retrievals after removing the spurious trends given above.   For SST, we use the Reynolds product.

The Measured – ORTM TA differences in Figures 5 and 6 are indicative of the spurious TA trends that are producing the drifts in the V8.0 AMSR-2 AS-ECVs.

Remote Sensing Systems
www.remss.com
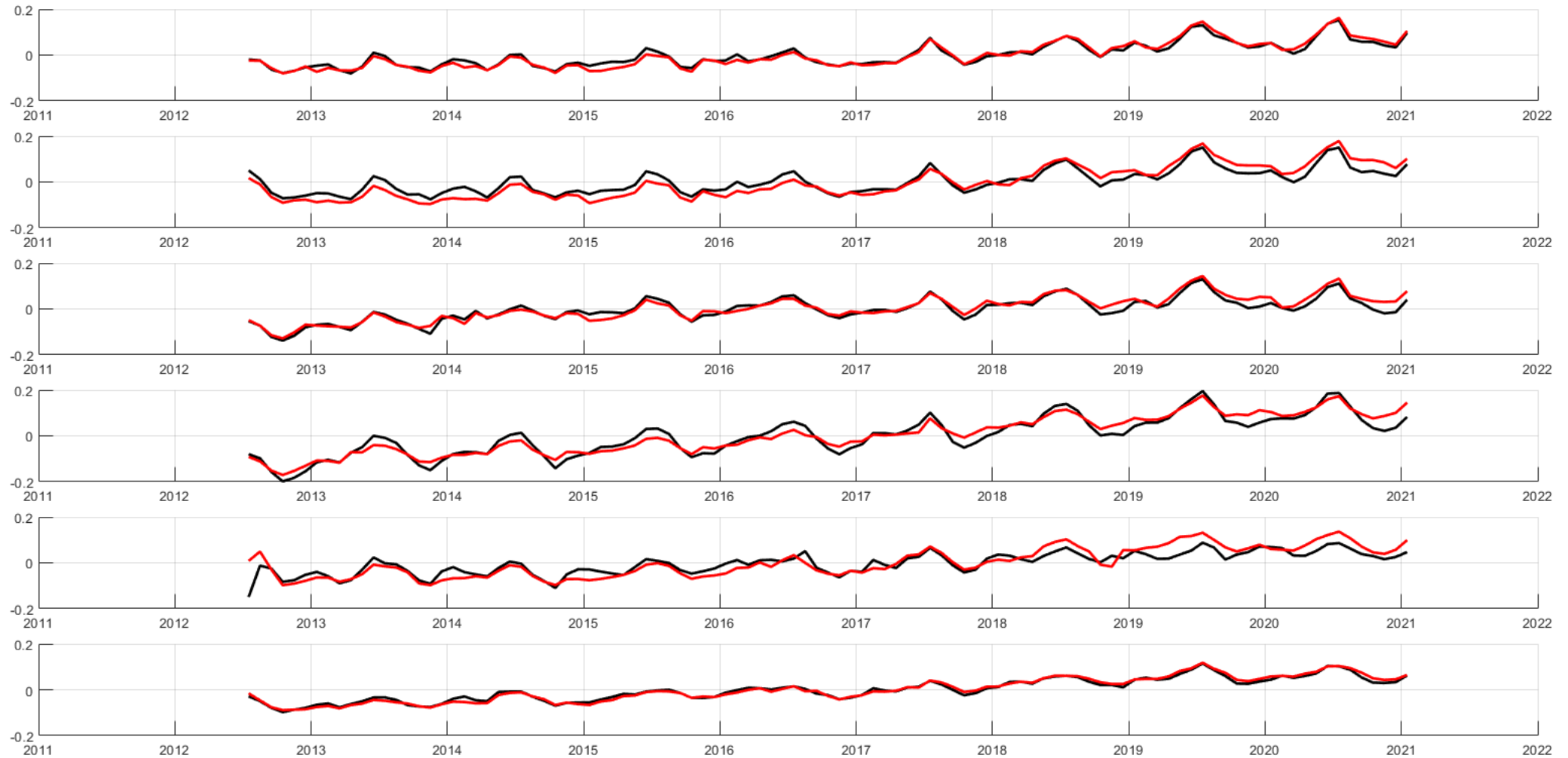
Fig. 5. V8.0 AMSR-2 Measured minus ORTM TA (K) for V-Pol channels. The black curves were created using ascending orbit segments (1:30 pm), and the red curves were created using descending orbit segments (1:30 am). The 6 frames from top to bottom are 6.9, 7.3, 10.7, 18.7, 23.8, and 36.5 GHz. The 89 GHz channels are not shown. An upward drift is apparent.

Remote Sensing Systems
www.remss.com
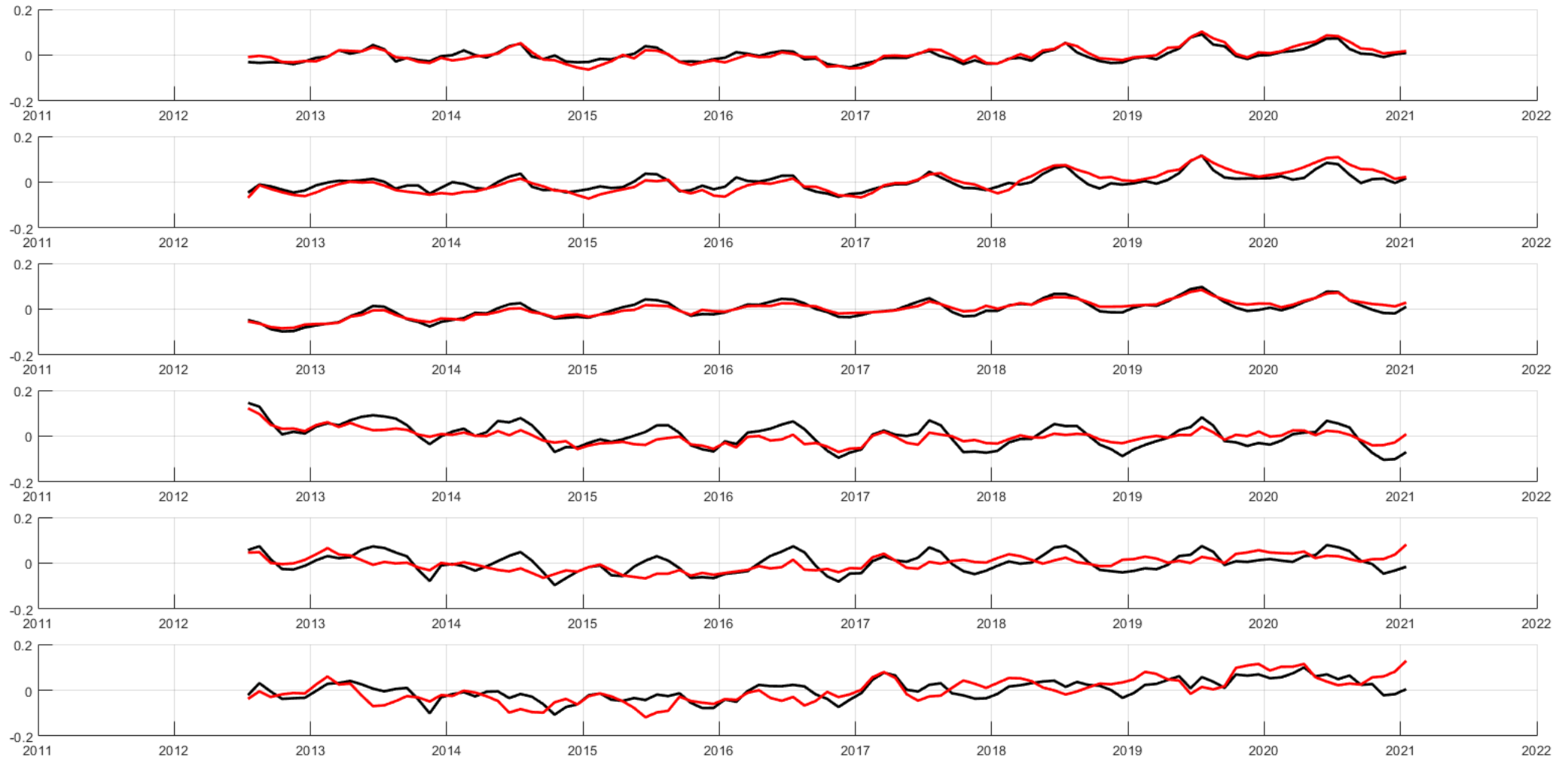
Fig. 6. Same as Figure 5 except the H-Pol channels are shown.

Possible Explanations for the TA Drifts: Earth Incidence Angle

We examined several possible explanations for the drifts in the AMSR-2 TAs. We first note that the drift in the V-Pol channels is positive and is larger than the H-Pol channels. This explains why the spurious SST trend is positive while the wind trend is negative.

Two potential explanations for the V-Pol trend being larger than the H-pol trend are:
1. An error in specifying the Earth incidence angle (EIA).
2. An error in specifying the hot load temperature.

We first examined the EIA hypothesis. A spurious drift in the reported EIA of -0.07 deg/decade would produce the observed trends in the V-Pol TA. An EIA error would also produce errors in the location of coastlines and islands. We did a detailed geolocation analysis looking at images of coastlines and islands from 2012 to 2020. This method can detect errors of 0.05 deg/decade in the EIA. We did not detect any geolocation errors in the TA imagery over the AMSR-2 mission.

Another argument against the EIA hypothesis is that the H-Pol TA for the lower frequencies would show a decreasing trend (i.e., opposite of the V-Pol trend). In fact, the H-Pol trends at the lower frequencies are positive, like the V-Pol trends, but much lower in magnitude.

We concluded that EIA is not the cause of the TA trends.

Remote Sensing Systems
www.remss.com

Possible Explanations for the TA Drifts: Hot Load

An error in specifying the hot load temperature could explain part of the observed TA drifts. Nearly all channels show positive trends with V-Pol being greater than H-Pol. In general, this behavior is consistent with a spurious trend in hot load. However, when examining the TA trends of the 12 channels in detail, one sees a lot of variation that is not consistent with a simple hot load error.

On average, the V-Pol TA trends indicate a hot-load drift error of about 0.30 K/decade, with the standard deviation among the 6 channels being 0.08 K/decade. However, the H-Pol TA trends are much smaller and indicate a hot-load drift error of 0.17 K/decade, with a large standard deviation of 0.18 K/decade.

To explore the hot-load hypothesis further, we performed a detailed analysis of TA trends over the Amazon Rainforest. The V8.0 AMSR-2 TA trends were compared to GMI and WindSat TA trends and to models. The Amazon TA measurements average about 270K. Because of this, they are very sensitive to any error in specifying the hot load temperature.   The Amazon analysis indicated a possible TA drift of about 0.1 K/decade: smaller than the ocean results but still significant.

Remote Sensing Systems
www.remss.com

Corrections to Hot Load Temperature Calculation

Investigating the hot load issue in even more detail, Figure 7 shows timeseries of the 10 thermistors attached to the hot load. In V8.0, the temperature of the hot load was calculated by averaging these 10 thermistors. However, during the daytime portion of the orbit, thermistor #7 drifts upwards relative to the other thermistors and exhibits a strong seasonal oscillation. For V8.2, we decided to exclude thermistor #7 from the average due to its anomalous behavior.

We also found another problem with the thermistor timeseries. Periodically, the AMSR-2 on-board Signal Processor Control unit (SPC) is switched from the A side to the B side. When this was last done in November 2017, we incorrectly specified the SPC offset used in the counts-to-temperature equation. This produced a 0.06 K spurious step in the timeseries. This is corrected in V8.2.

The combined effect of removing thermistor #7 from the hot load average and correcting the SPC problem resulted in a 0.1 K/decade decrease in the hot load trends. This brought the AMSR-2 TAs into good agreement with WindSat and GMI over the Amazon Rainforest. However, over the colder oceans, this change has little effect. It only decreases the V-pol trends by 0.05 K/decade and the H-Pol trends by 0.02 K/decade.

Correcting the way in which the hot-load temperature is calculated provided better agreement with WindSat and GMI over the Amazon Rainforest, but provided little improvement over the oceans.

Remote Sensing Systems
www.remss.com
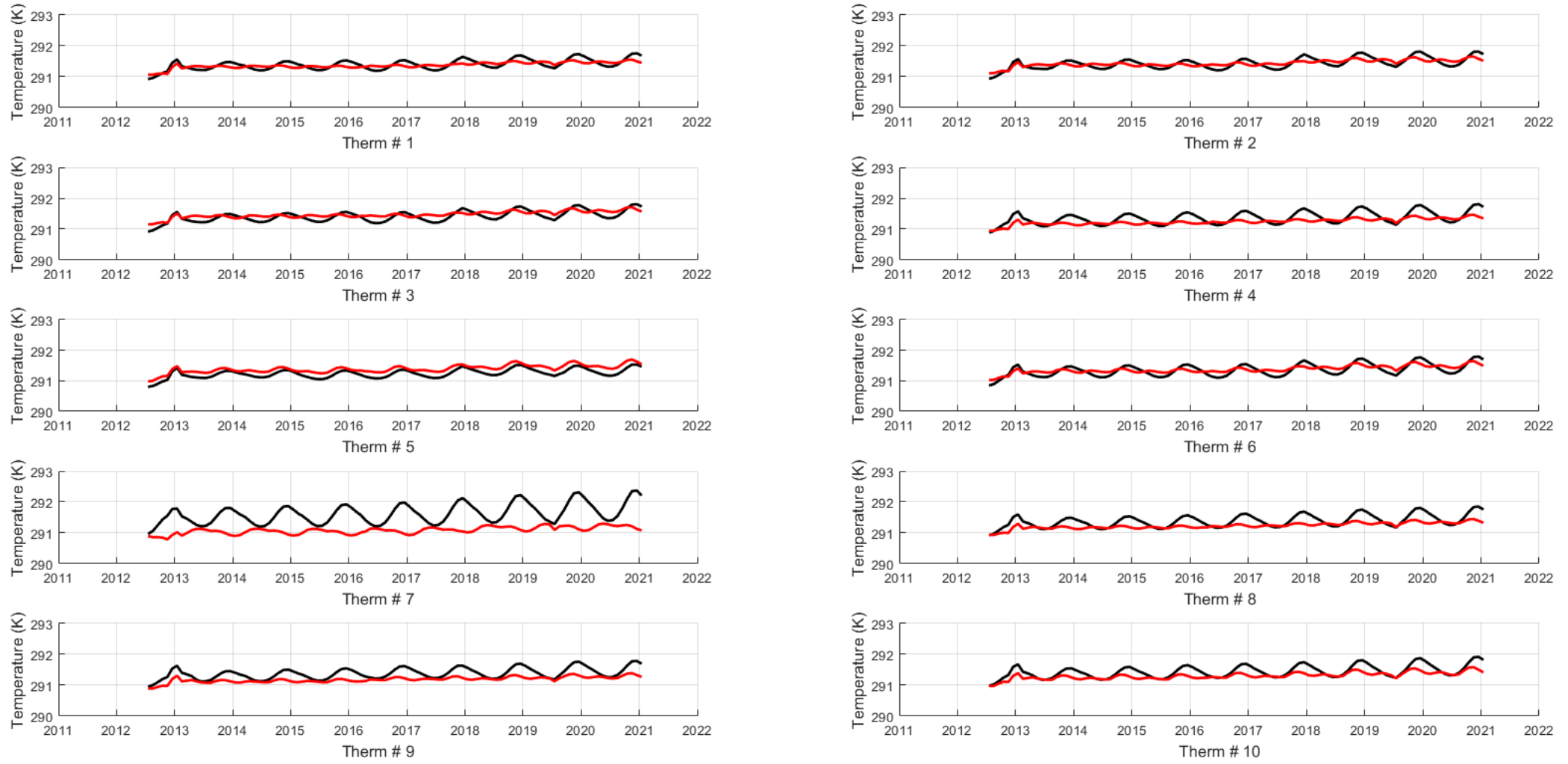
Fig. 7. Timeseries of the 10 thermistors attached to the AMSR-2 hot load. Black curves correspond to ascending orbit segments (1:30 pm) and red curves correspond to descending orbit segments (1:30 am). Thermistor #7 is anomalous and is excluded in V8.2.

Remote Sensing Systems
www.remss.com

Adjusting the Non-Linearity Coefficients of the AMSR-2 Receivers

One remaining explanation for the TA drifts over the ocean is that the non-linearity responses of the AMSR-2 receivers are drifting. The internal temperatures of the AMSR-2 Signal Processor Control Unit (SPC) have been changing significantly over time. We hypothesize that the non-linear characteristics of the AMSR-2 receivers have slightly changed due to the changes in the SPC temperatures. We found two thermistors that correlated well with the TA drifts shown in Figures 5 and 6: SPC Thermistor #3 (HTS control temperature 3) and SPC Thermistor #17 (SPC A temperature).

The dTA timeseries in Figures 5 and 6 are regressed versus the T_3 and T_{17} timeseries as follows:

$$dTA = a + b*T_3 + c*T_{17}$$

The a, b, and c coefficients are found for each of the 16 AMSR-2 channels. The non-linearity correction is then applied as:

$$TAcorrected = TA - (TA-T_{cold})(T_{hot}-TA)*dTA/A$$

where T_{cold} is the temperature observed by the cold-space mirror and T_{hot} is temperature of the hot load. The term A is the average value of $(TA-T_{cold})(T_{hot}-TA)$ over the oceans for a given channel.

Remote Sensing Systems
www.remss.com

Results After Applying the Non-Linearity Correction

Figures 8 and 9 show the TA trends after applying the hot load and non-linearity correction. For reference, we have also inserted Figures 5 and 6 from above, which show the results before applying the corrections. Comparing the figures, one sees that in addition to removing the long-term drifts in the TAs, the corrections also remove the seasonal variations in the TA measured minus TA ORTM differences. Comparison with the GPM Microwave Imager (GMI) (not shown here) also show that these seasonal variations in V8.0 are spurious.

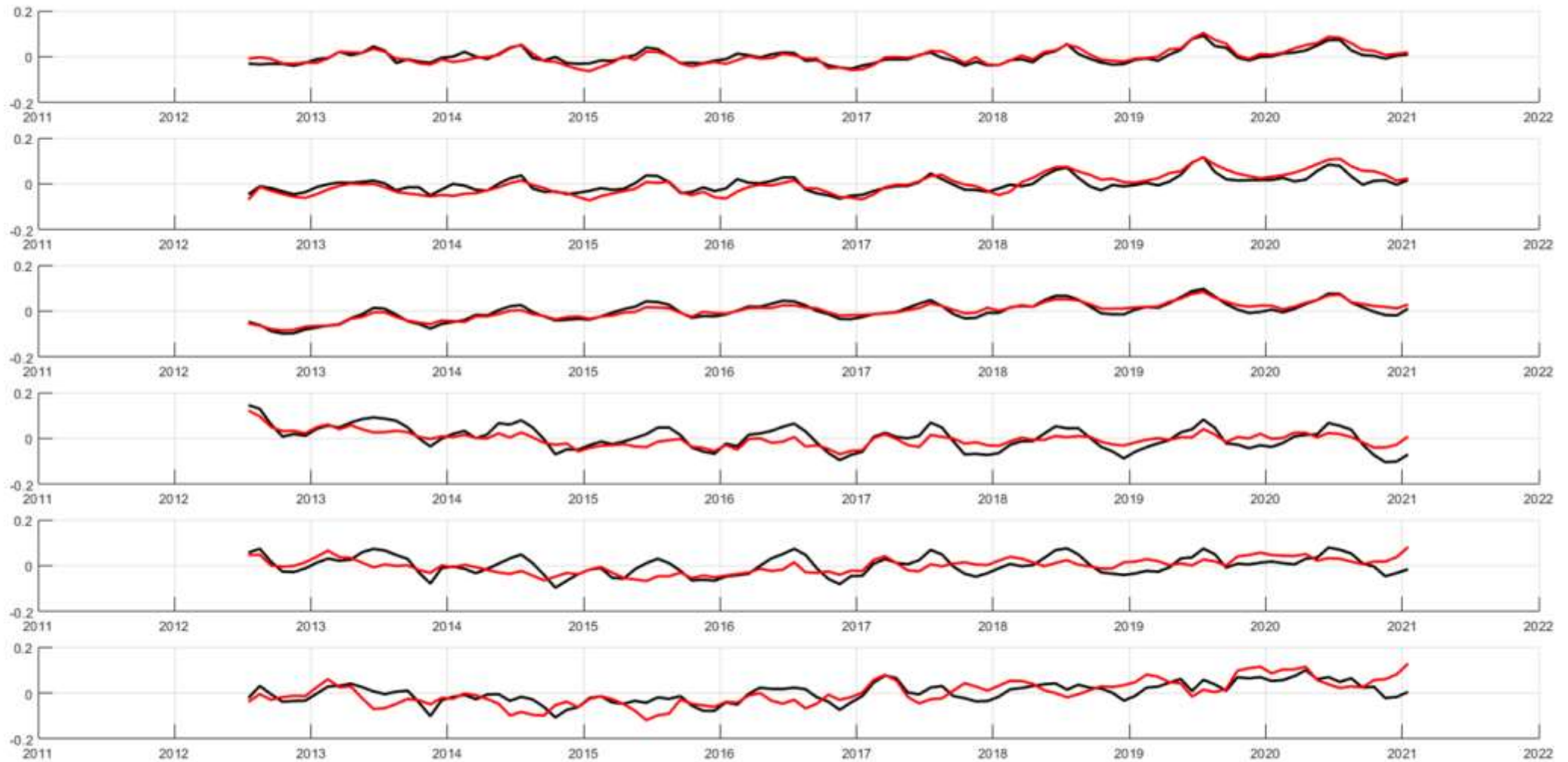Remote Sensing Systems
www.remss.com
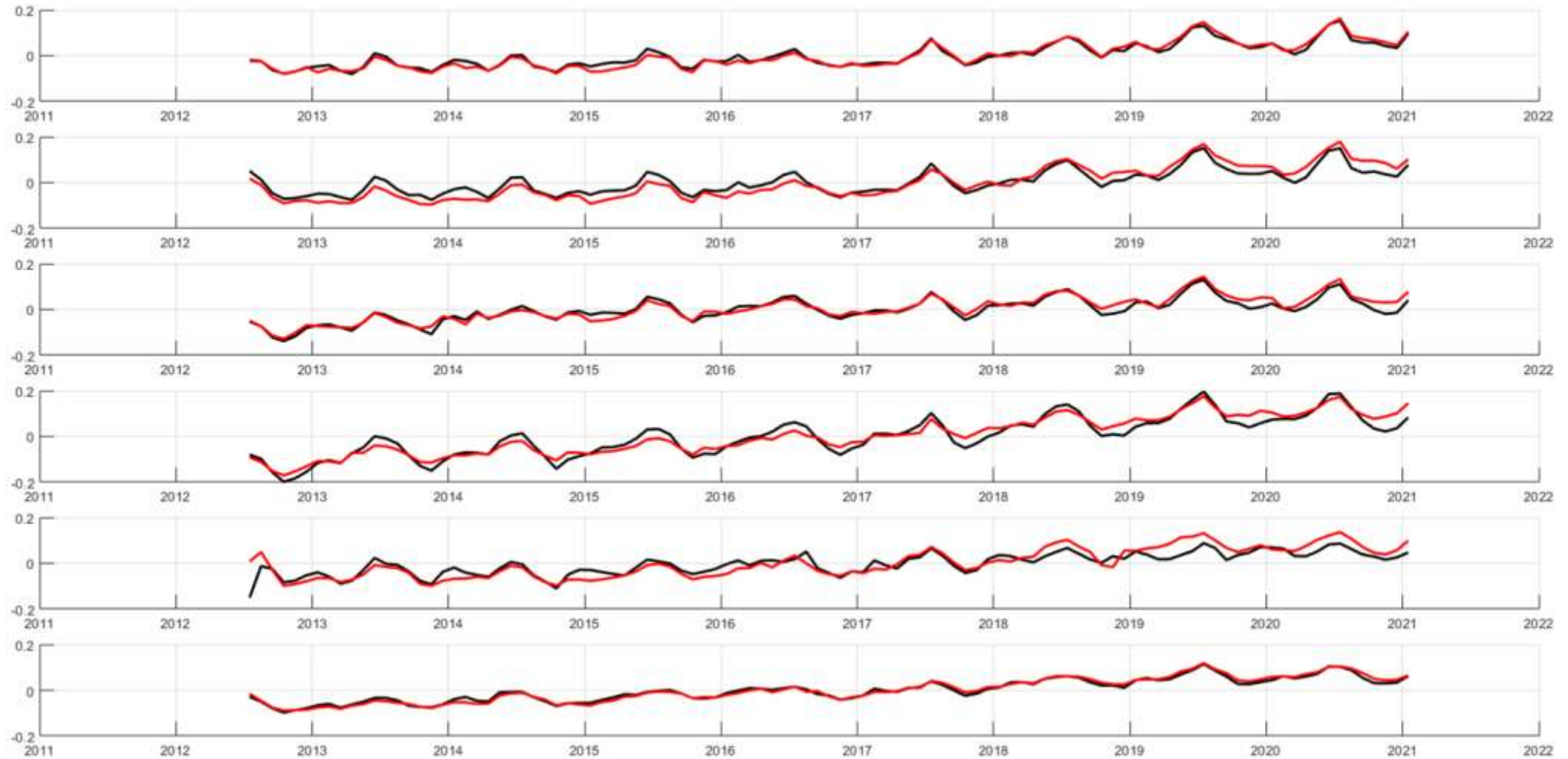
Fig. 5 (from above). V8.0 AMSR-2 Measured minus ORTM TA (K) for V-Pol channels. Black curves correspond to ascending orbit segments (1:30 pm) and red curves correspond to descending orbit segments (1:30 am). The 6 frames from top to bottom are 6.9, 7.3, 10.7, 18.7, 23.8, and 36.5 GHz. The 89 GHz channels are not shown. An upward drift is apparent.
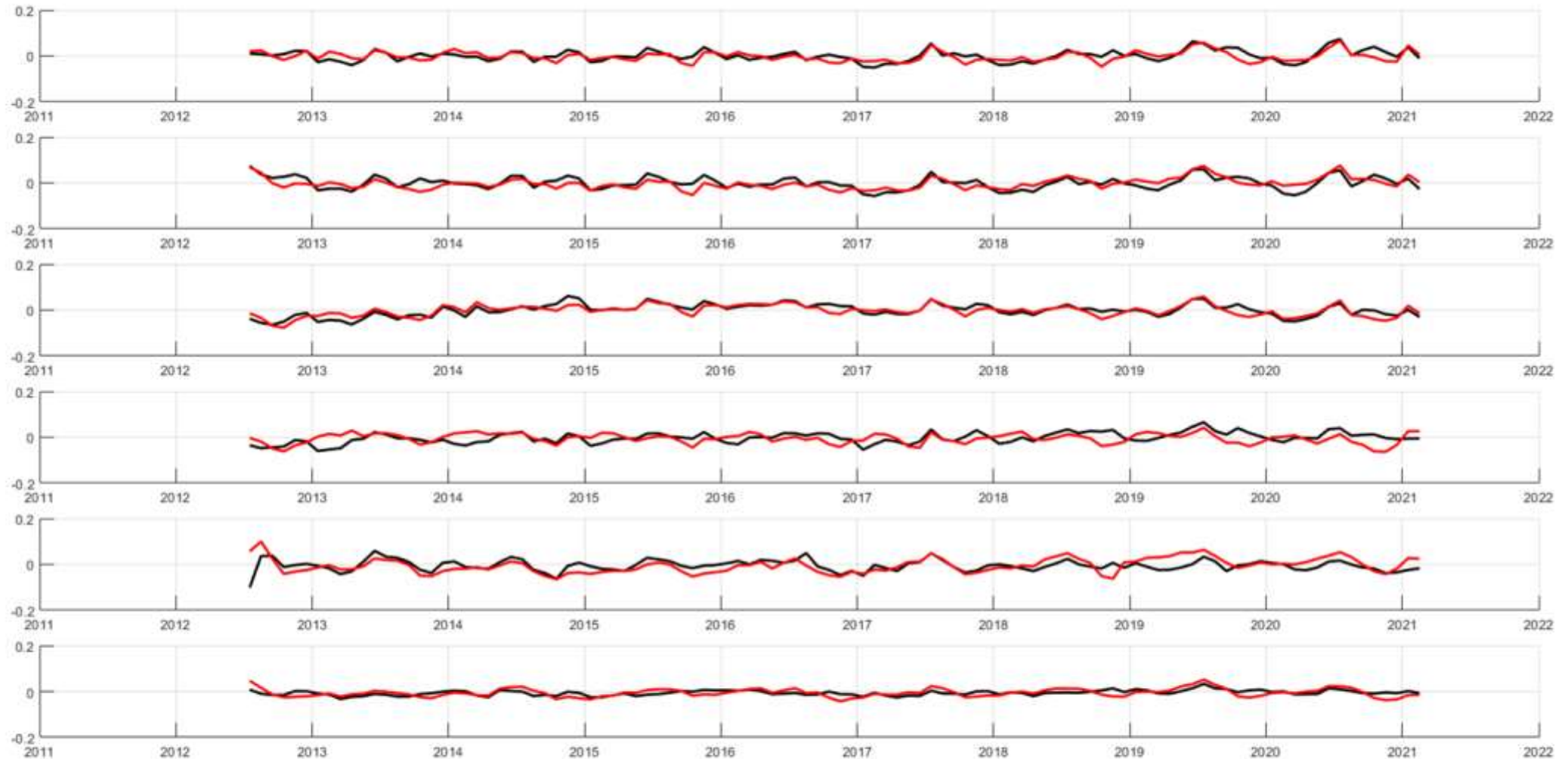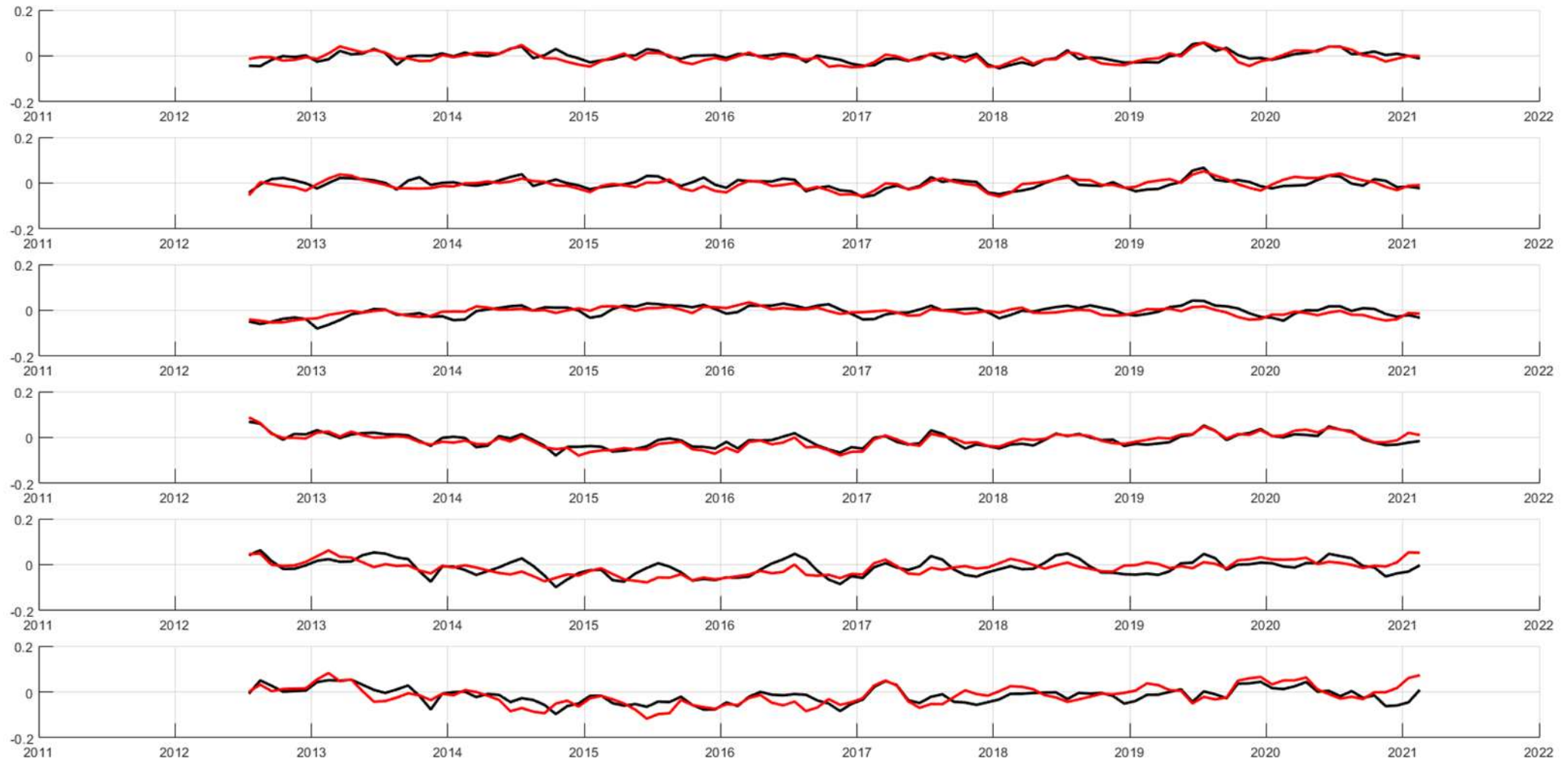
Fig. 8. V8.2 AMSR-2 Measured minus ORTM TA (K) for V-Pol channels. Black curves correspond to ascending orbit segments (1:30 pm) and red curves correspond to descending orbit segments (1:30 am). The 6 frames from top to bottom are 6.9, 7.3, 10.7, 18.7, 23.8, and 36.5 GHz. The upward drift is gone.

Remote Sensing Systems
www.remss.com

Fig. 6 (from above). V8.0 AMSR-2 Measured minus ORTM TA (K) for H-Pol channels. Black curves correspond to ascending orbit segments (1:30 pm) and red curves correspond to descending orbit segments (1:30 am). The 6 frames from top to bottom are 6.9, 7.3, 10.7, 18.7, 23.8, and 36.5 GHz. The 89 GHz channels are not shown. Drifts and seasonal oscillations are apparent.

Remote Sensing Systems
www.remss.com

Fig. 9. V8.2 AMSR-2 Measured minus ORTM TA (K) for H-Pol channels. Black curves correspond to ascending orbit segments (1:30 pm) and red curves correspond to descending orbit segments (1:30 am). The 6 frames from top to bottom are 6.9, 7.3, 10.7, 18.7, 23.8, and 36.5 GHz. Drifts are gone and seasonal oscillations are diminished.

Remote Sensing Systems
www.remss.com

Conclusions

The spurious drifts in the V8.0 AMSR-2 AS-ECVs have been removed by:

1. Correcting the way in which the hot-load temperature is calculated.
2. Making the non-linearity coefficients a function of the SPC temperatures.

In the future, we will carefully monitor the AMSR-2 performance relative to the GPM Microwave Imager (GMI) to verify the V8.2 AS-ECVs remain stable over time.

Remote Sensing Systems
www.remss.com